

ELECTRONIC SUPPLEMENTARY INFORMATION

Multi-dyes@MOF composite boosts highly efficient photodegradation of ultra-stubborn dye of reactive blue 21 under visible-light irradiation

Qing Li,^{ab‡} Zeng-Lu Fan,^{b‡} Dong-Xu Xue,*^a Yu-Feng Zhang,^a Zong-Hui Zhang,^a Qian Wang,^a Hua-Ming Sun,^a Ziwei Gao*^a and Junfeng Bai^{ac}

^a Key Laboratory of Applied Surface and Colloid Chemistry, Ministry of Education, School of Chemistry & Chemical Engineering, Shaanxi Normal University, Xi'an 710062, P. R. China.

E-mail: xuedx@snnu.edu.cn; zwgao@snnu.edu.cn

^b College of Environmental & Chemical Engineering, Xi'an Polytechnic University, Xi'an 710048, P. R. China.

^c State Key Laboratory of Coordination Chemistry, School of Chemistry & Chemical Engineering, Nanjing University, Nanjing 210093, P. R. China.

‡ These authors contributed equally to this work.

Table of Contents

Section S1 Reported decoloration / degradation performances towards RB21.....	S2-S3
Section S2 PXRD characterizations of 1	S4
Section S3 UV-Vis calibration curves for organic dyes.....	S5-S6
Section S4 Adsorption of dyes over 1	S7-S9
Section S5 Adsorption capacity, efficiency and kinetic of mixed dyes over 1	S9-S10
Section S6 Adsorption kinetics determination.....	S11
Section S7 UV-Vis DRS for pure dyes, 1 and single-dye@ 1	S12
Section S8 UV-Vis DRS for dual/triple-dyes@ 1	S13
Section S9 The band gaps of fresh and single/dual/triple-dyes sensitized 1	S14
Section S10 UV-Vis DRS, band gaps of 1 and RB21/1	S15
Section S11 Calculation methods for band gaps.....	S16
Section S12 The photocatalytic degradation performance of P25.....	S17
Section S13 Photocatalytic degradation performances and recyclability.....	S18
Section S14 COD _{cr} determinations.....	S19
Section S15 References.....	S20

Section S1 Reported decoloration / degradation performances towards RB21

Table S1 Performance summary of the RB21 decoloration / degradation in the presence of reported different catalysts

Catalysts	Efficiency and reactive time	Temp. /K	Conc. dyes (mg L ⁻¹)	Vol. dyes (mL)	Aiders	Conc. Catalysts	Products	Light source	Ref.
Cellobiose dehydrogenase (CDH) and Laccases	37.19% in 12 h	n.a.	25	20	H ₂ O ₂ , 50 to 200 μM	CDH, 0.1 U/mL Laccase, 0.5 U/mL	Small molecular compounds	—	[1]
Turnip peroxidase	57.00% in 50 min	303	50	1.5	H ₂ O ₂ , 100 μM/L	10.83 U/mL	Small molecular compounds	—	[2]
Horseradish peroxidase	59.00% in 45 min	298	100	100	H ₂ O ₂ , 2 × 10 ⁻³ mM/L	29.85 U/mL	—	—	[3]
Cyathus bulleri Laccase	35% in 5 h	n.a.	100	20	ABTS, 100 μM	100 mU/mL	Small molecular compounds	—	[4]
TiO ₂ (P-25)/near UV	67.58% in 2 h	303	75	100	—	1 mg/mL	Mineralization	UV	[5]
Fenton	62.70% in 2 h	n.a.	75	100	H ₂ O ₂ , 5 × 10 ⁻³ M	Fe ²⁺ and Fe ³⁺ , 5 × 10 ⁻⁴ M	Mineralization	—	[5]
Fenton/near-UV	67.70% in 2 h	n.a.	75	100	H ₂ O ₂ , 5 × 10 ⁻³ M	Fe ²⁺ and Fe ³⁺ , 5 × 10 ⁻⁴ M	Mineralization	UV	[5]
Fenton-like	60.10% in 2 h	n.a.	75	100	H ₂ O ₂ , 5 × 10 ⁻³ M	Fe ²⁺ and Fe ³⁺ , 5 × 10 ⁻⁴ M	—	—	[5]
Fenton-like/near-UV	76.30% in 2 h	n.a.	75	100	H ₂ O ₂ , 5 × 10 ⁻³ M	Fe ²⁺ and Fe ³⁺ , 5 × 10 ⁻⁴ M	Mineralization	UV	[5]
Soybean peroxidase	96.00% in 4 h	298	200	—	H ₂ O ₂ , 9.98 × 10 ⁻⁵ M	2.06 × 10 ⁻⁷ M	Small molecular compounds	—	[6]
Phanerochaete chrysosporium	97.00% in 6 d	n.a.	200	—	—	—	Small molecular compounds	—	[7]
Pellet-supported Pd	> 95% in about 72 d	295	500	—	—	4 mg/mL	Small molecular compounds	—	[8]
(MB+BY24+BR14)@1	95.36% in 8 h	298	47.54	60	—	0.083 mg/mL	Mineralization	Visible	This work

ABTS: 2,2'-Azino-Bis(3-Ethylbenzothiazoline-6-Sulfonic Acid); Small molecular compounds include: O-Xylene, 2,3-Dihydro-1H-isoindole, Isoindole-1,3-dione, 6-Hydroxy-2,3-dihydro-isoindol-1-one, 4-Hydroxy-phthalic acid, 2-BenzeneSulfonyl-ethanol, (4-Hydroxy-phenyl)-sulfamic acid, 2,3-Dihydro-1H-isoindole-5-sulfonic acid, 1-Amino-3-imino-3H-isoindole-5-sulphonic acid, 1,3-Dioxo-2,3-dihydro-1H-isoindole-5-sulphonic acid, 3,4-Dicarbamoyl-benzenesulfonic acid, 1-Amino-3-(N-aminomethyl-formimidoylamino)-2,3-dihydro-1H-isoindole-5-sulfonic acid, 3-Amino-1-(3-amino-6-hydroxy-2,3-dihydro-1H-isoindole-1-ylimino)-2,3-dihydro-1H-isoindole-5-sulfonic acid, 1-Amino-3-(3-amino-2,3-dihydro-isoindole-1-ylideneamino)-2,3-dihydro-1H-isoindole-5-sulfonic acid, 3-[5-(4-Hydroxy-phenylsufamoyl)-isoindole-1-ylideneamino]-1H-isoindole-5-sulfonic acid.

Section S2 PXRD characterizations of **1**

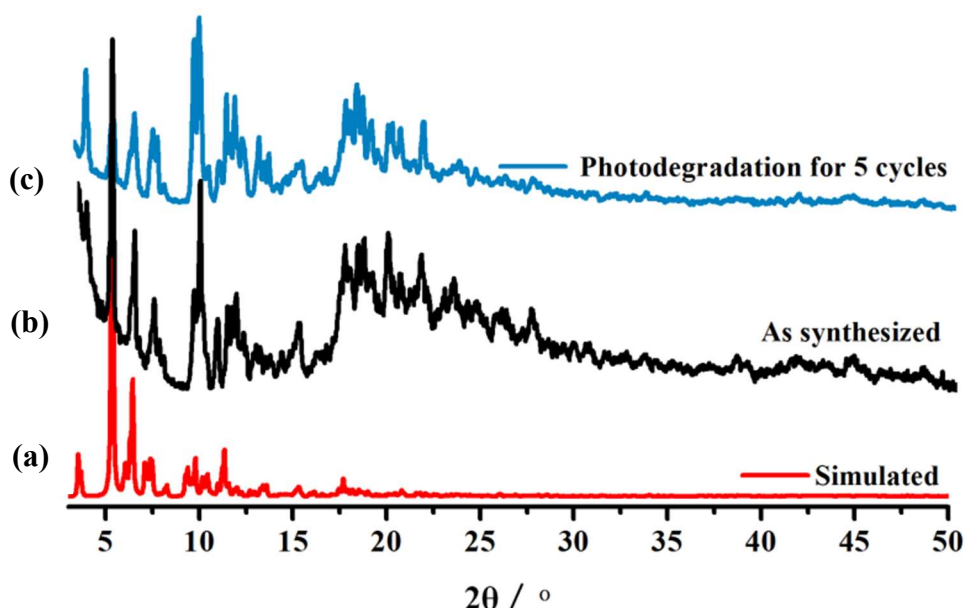
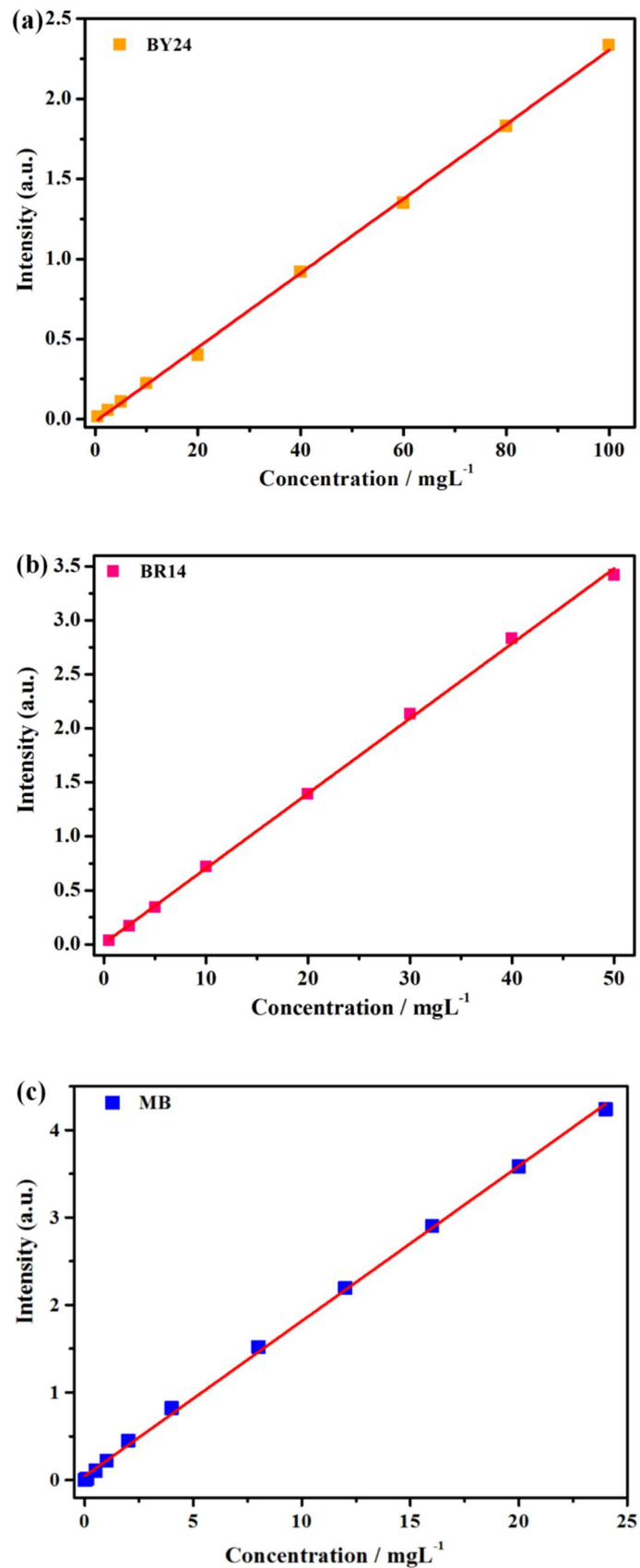


Fig. S1 PXRD patterns of simulated (a), as-synthesized **1** (b) and (**MB + BR14 + BY24**)@**1** (c) after photodegradation RB21 for 5 cycles.

Section S3 UV-Vis calibration curves for organic dyes



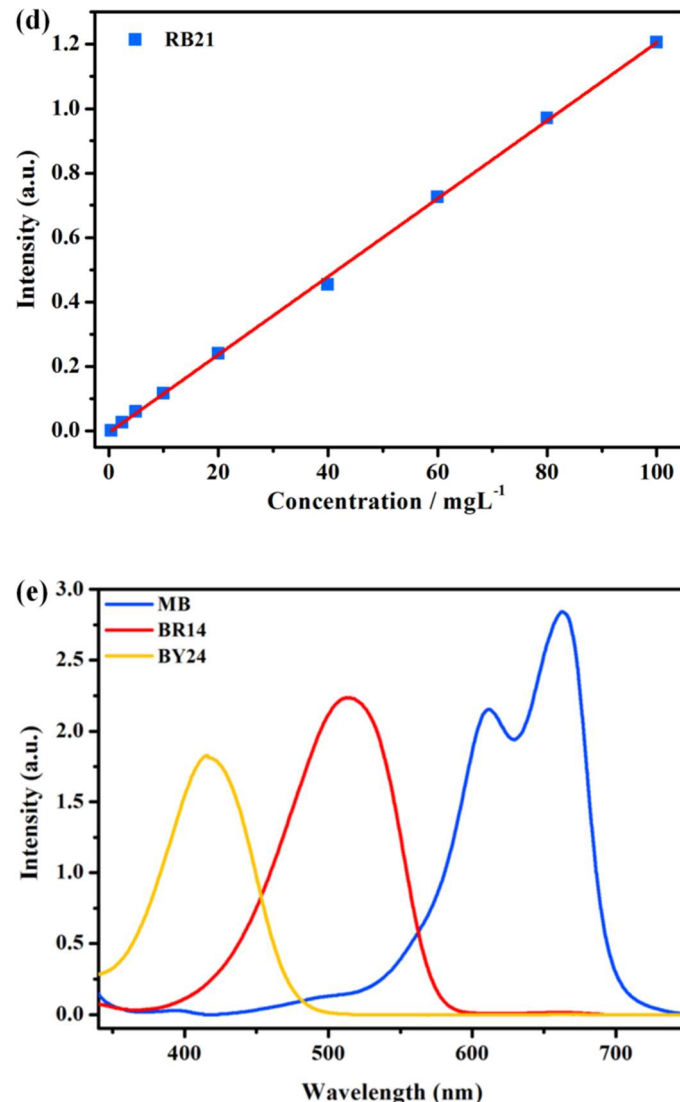


Fig. S2 UV-Vis calibration curves for dyes BY24 (a, $R^2 = 0.999$), BR14 (b, $R^2 = 0.999$), MB (c, $R^2 = 0.999$) and RB21 (d, $R^2 = 0.999$); UV-Vis characteristic absorption bands for BY24 ($\lambda_{\text{max}} = 420$ nm), BR14 ($\lambda_{\text{max}} = 520$ nm) and MB ($\lambda_{\text{max}} = 664$ nm) (e).

Section S4 Adsorption of dyes over **1**

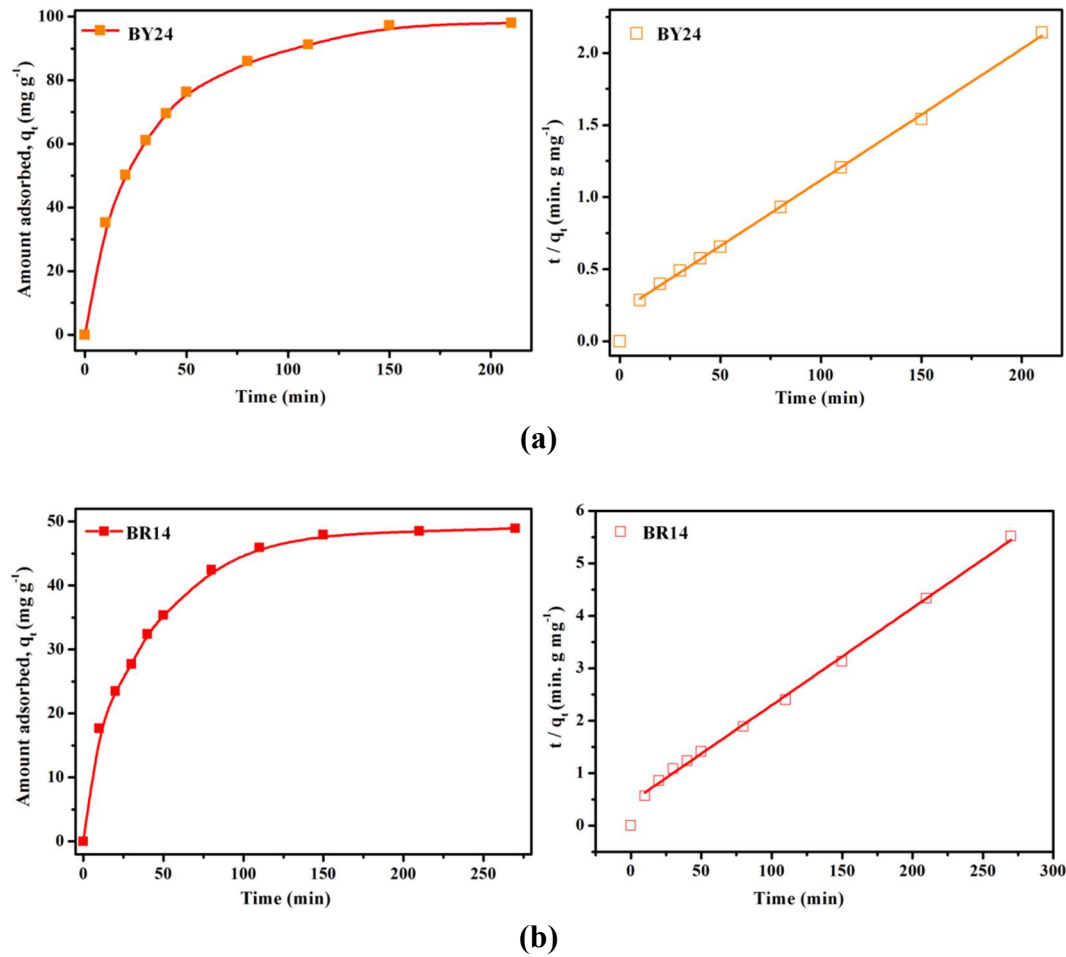


Fig. S3 Adsorption kinetics and corresponding kinetic data fitting of BY24 (a, $R^2 = 0.999$), BR14 (b, $R^2 = 0.998$) adsorption over **1** using the pseudo-second-order kinetics model.

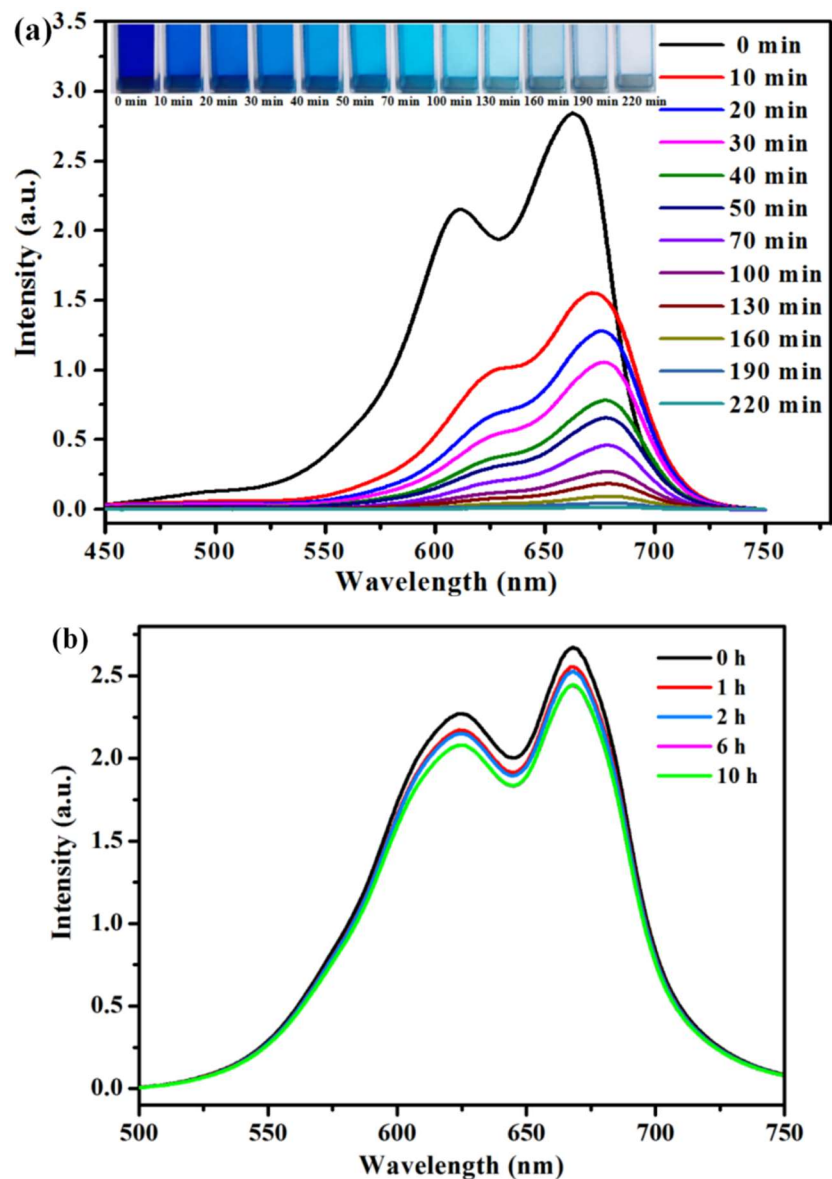
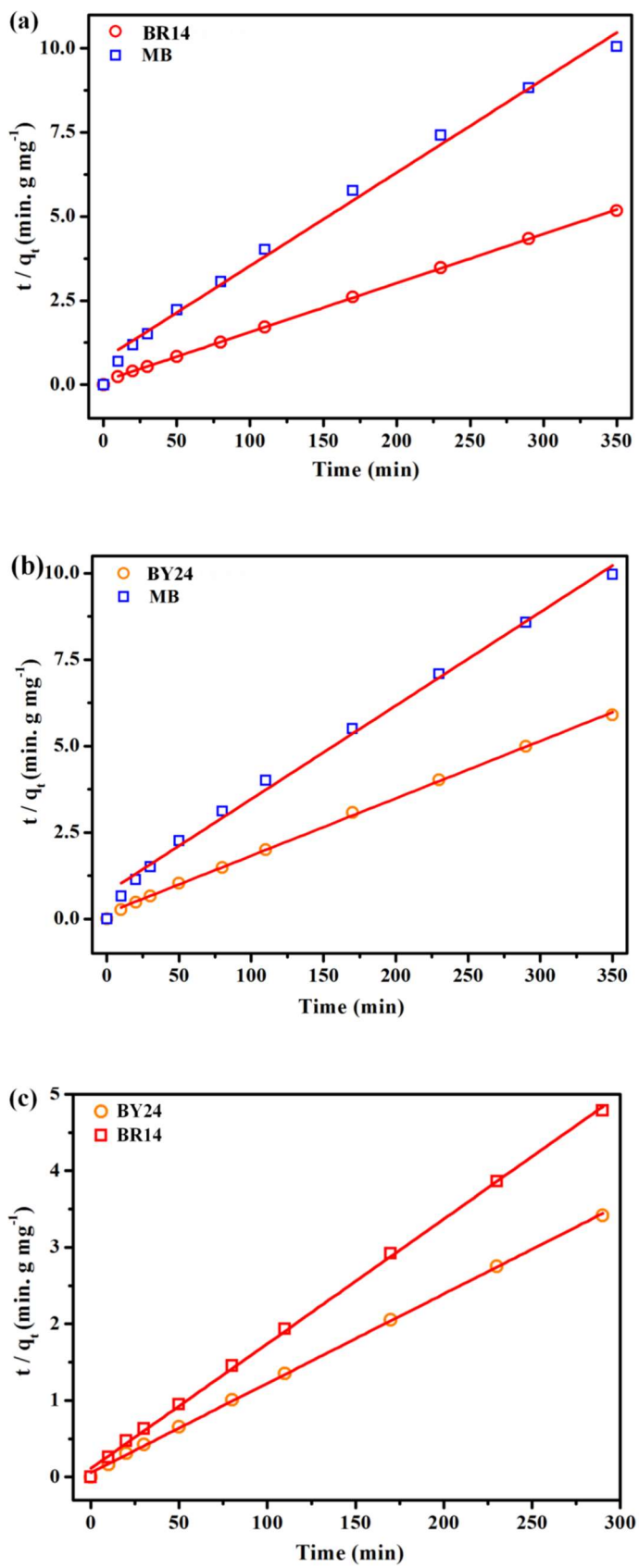


Fig. S4 Sequential UV-Vis spectra changes of MB (a) and RB21 (b) aqueous solution in the presence of **1**.

Section S5 Adsorption capacity, efficiency and kinetic of mixed dyes over 1



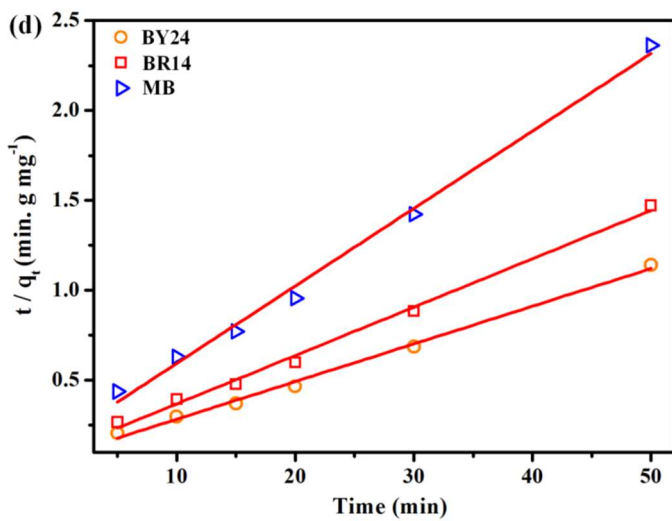


Fig. S5 Kinetic data fitting of dual-dyes containing (a) MB ($R^2 = 0.994$) + BR14 ($R^2 = 0.999$), (b) MB ($R^2 = 0.995$) + BY24 ($R^2 = 0.999$), (c) BR14 ($R^2 = 0.999$) + BY24 ($R^2 = 0.999$) and triple-dyes containing (d) MB ($R^2 = 0.993$) + BR14 ($R^2 = 0.993$) + BY24 ($R^2 = 0.994$) adsorption over **1** using the pseudo-second-order kinetics model.

Table S2 Adsorption capacity, efficiency and adsorption rate constant of **1** towards mixed dyes.

Dual/triple mixed dyes	Concentration/mg L ⁻¹		Capacity mg g ⁻¹	Efficiency %	Rate Constants g mg ⁻¹ min ⁻¹	R^2
	Original	Finished				
MB+BY24	MB	18.02	0.464	59.37	97.43	0.02704
	BY24	31.70	2.017	35.11	93.64	0.01660
MB+BR14	MB	18.29	0.888	34.80	95.15	0.02777
	BR14	34.59	0.768	67.65	97.78	0.01458
BY24+BR14	BY24	45.27	2.75	84.88	93.93	0.01167
	BR14	31.23	0.93	60.61	97.03	0.01628
MB+BY24+BR14	MB	14.15	0.089	21.16	99.37	0.04308
	BY24	28.43	0.768	43.82	97.30	0.02094
	BR14	22.69	0.072	33.96	99.68	0.02688

Section S6 Adsorption kinetics determination

$$\frac{dq_t}{dt} = k_2(q_e - q_t)^2 \quad \text{or} \quad \frac{t}{q_t} = \frac{1}{k_2 q_e^2} + \frac{1}{q_e} t \quad (1)$$

The second order kinetic constant k_2 could be determined by treating the changes of adsorbed amount with time with the pseudo-second-order kinetic model ($k_2 = \text{slope}^2 / \text{intercept}$ while t/q_t is plotted against t ; q_t represents the adsorption quantity changing with time).⁹

Section S7 UV-Vis DRS for pure dyes, **1 and single-dye@**1****

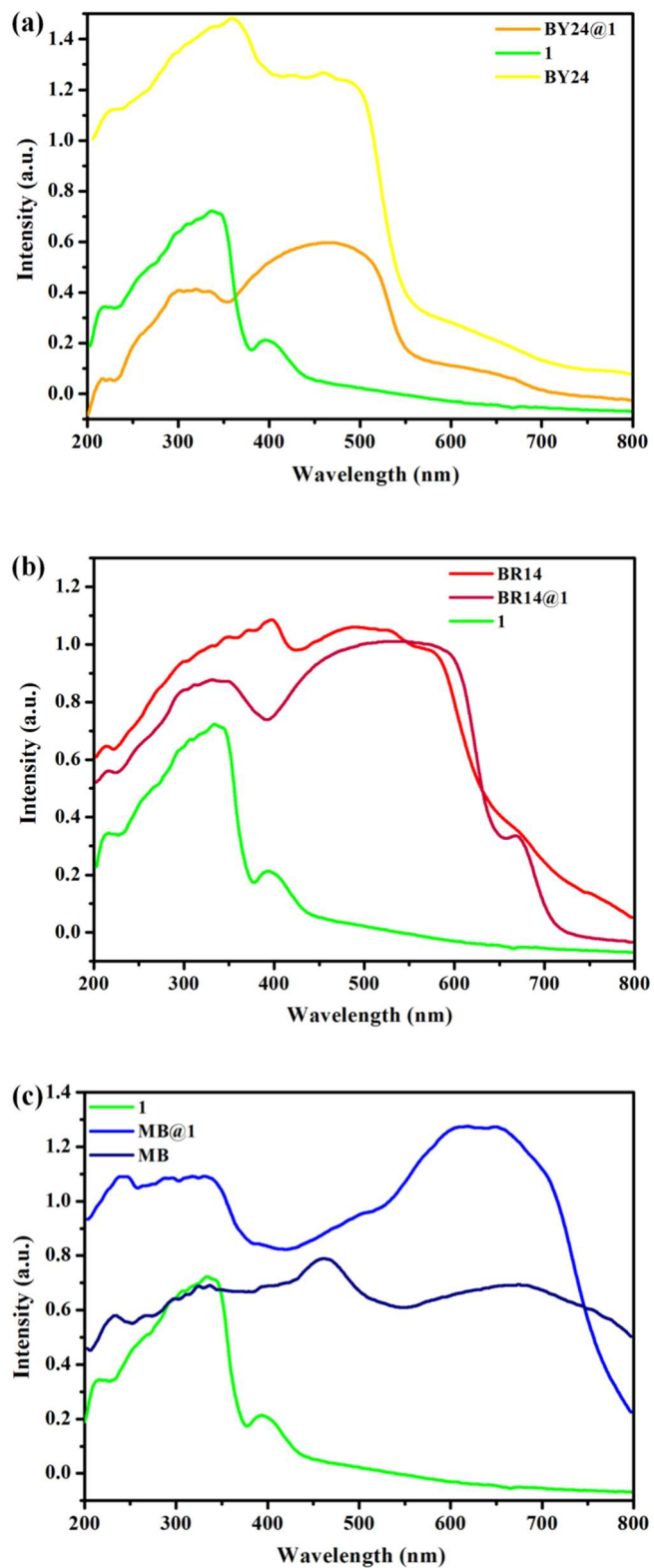


Fig. S6 UV-Vis diffuse reflectance spectra of as-synthesized **1**, pure BY24 (a), BR14 (b), MB (c) and corresponding dye@MOF composites.

Section S8 UV-Vis DRS for dual/triple-dyes@1

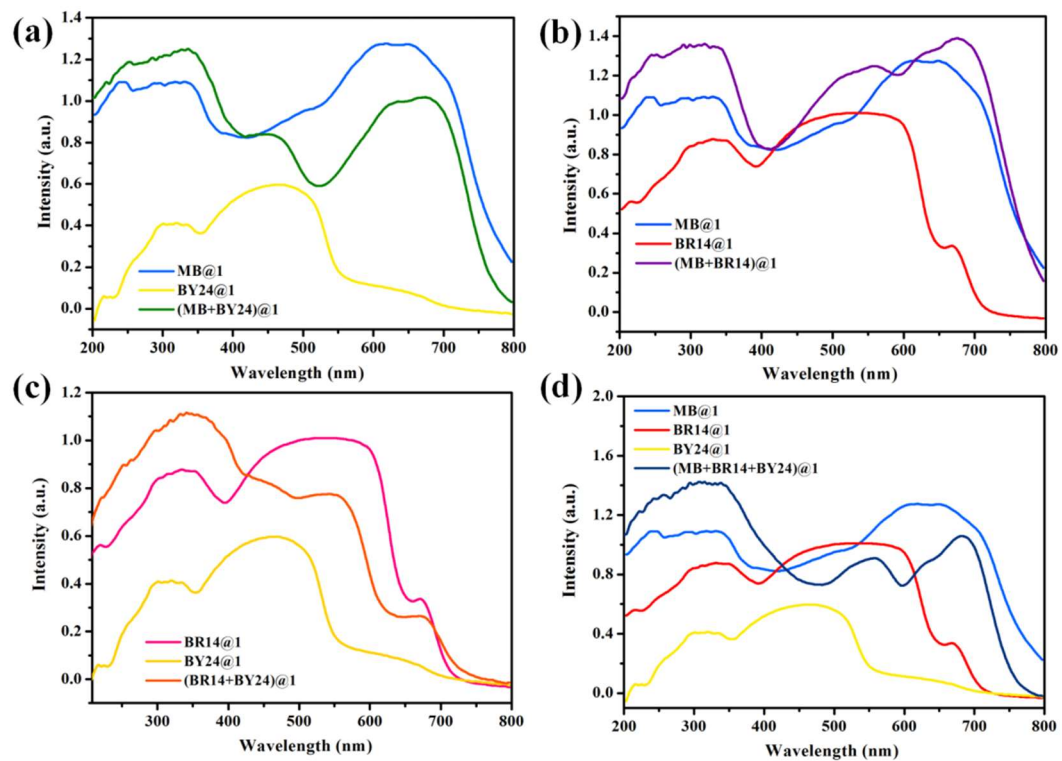


Fig. S7 UV-Vis diffuse reflectance spectra of **(MB + BY24)@1** (a), **(MB + BR14)@1** (b), **(BY24 + BR14)@1** (c), **(MB + BY24 + BR14)@1** (d) and their corresponding team Members.

Section S9 The band gaps of fresh and single/dual/triple-dyes@1

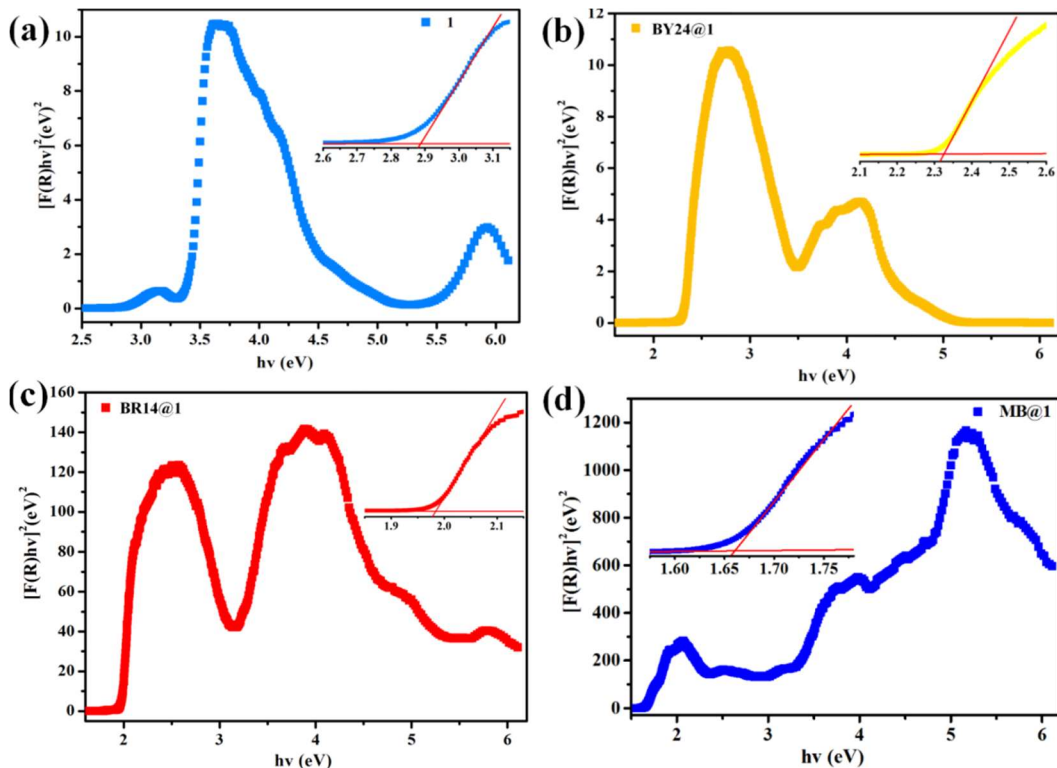


Fig. S8 The energy band gaps of as-synthesized **1** (a), **BY24@1** (b), **BR14@1** and **MB@1** (d).

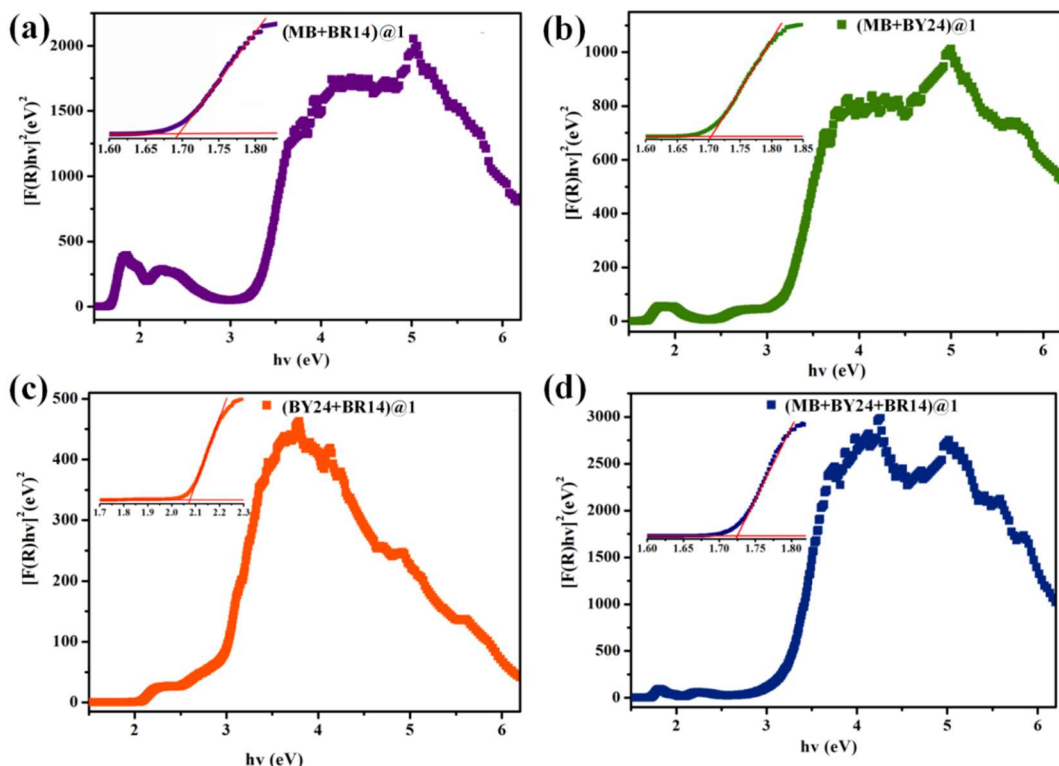


Fig. S9 The energy band gaps of **(MB + BR14)@1** (a), **(MB+BY24)@1** (b), **(BY24 + BR14)@1** (c) and **(MB + BY24 + BR14)@1** (d).

Section S10 UV-Vis DRS, band gaps of **1 and **RB21/1****

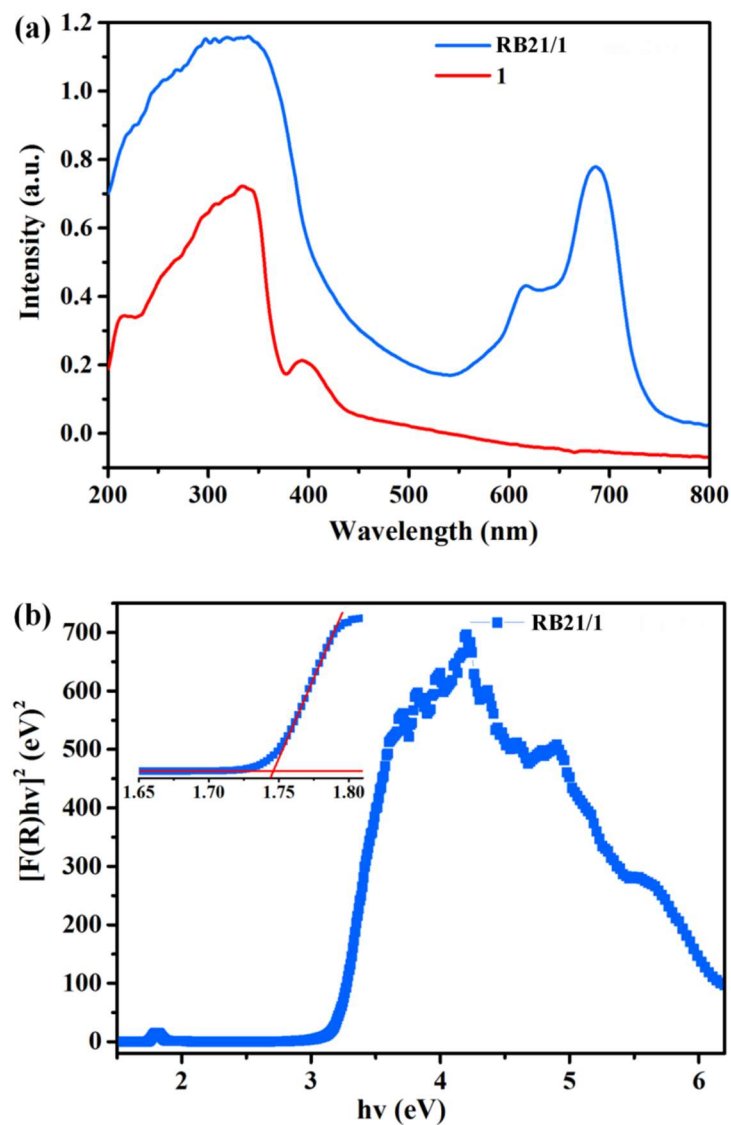


Fig. S10 UV-Vis diffuse reflectance spectra of **1**, **RB21/1** (a) and corresponding band gaps of **RB21/1** (b)

Section S11 Calculation methods for band gaps

It has been confirmed that the optical band gaps (E_g) of catalysts play key roles in affecting the efficiency of photocatalysis elimination process of organic dyes and usually catalysts with narrower band gaps would be more conducive to the separation of the charges.¹⁰ Popularly, the optical radiation with energy larger than the band gaps of photocatalyst would run more efficiently in photocatalytic reaction.^{11, 12}

The calculations of band gaps for as-synthesized and single/dual/triple-dyes sensitized **1** were studied through the detection of their UV-Vis diffuse reflectance spectra (UV-Vis DRS). According to the Kubelka-Munk equation $F(R) = \alpha = (1-R)^2 / 2R$ and transformed Kubelka-Munk formula $[F(R)hv]^2 = A(hv - Eg)$, where R, α , hv, Eg and an orderly represent the percentage of reflected light, optical absorption coefficient, energy of incident photon, the band gap energy and transition probability rate constants, Eg values were obtained from the plots of Kubelka-Munk function $[F(R)hv]^2$ versus hv and precisely determined as the abscissa values of intersection between the tangent line of energy axis and the line extrapolated from the linear portion of the adsorption edge.^{11, 12}

Section S12 The photocatalytic degradation performance of P25

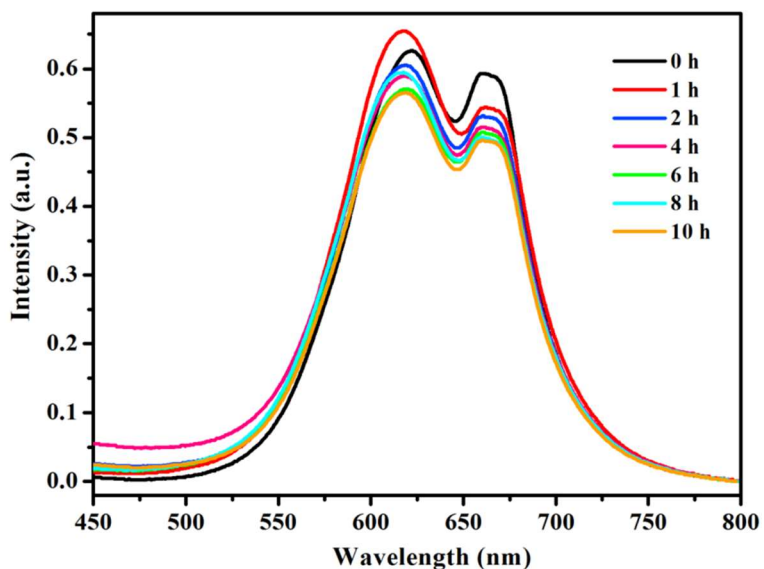


Fig. S11 Sequential UV-Vis spectra changes of RB21 aqueous solution under visible-light irradiation in the presence of P25.

Section S13 Photocatalytic degradation performances and recyclability

Table S3 Photocatalytic degradation performances towards RB21.

Catalysts	Efficiency (%)	Reaction rate constant (h ⁻¹)	Conc. Organic dyes (mg L ⁻¹)		<i>R</i> ²
			Start	End	
RB21/1	73.13%@10 h	0.112	47.54	12.77	0.988
MB@1	91.37%@10 h	0.228	47.54	4.10	0.996
BR14@1	88.76%@10h	0.215	47.54	5.34	0.985
BY24 @1	40.99%@10h	0.043	47.54	28.05	0.991
(MB + BR14)@1	33.87%@10h	0.026	47.54	31.44	0.980
(MB + BY24)@1	93.10%@10h	0.239	47.54	3.28	0.993
(BR14 + BY24)@1	89.98%@10h	0.198	47.54	4.76	0.997
(MB + BR14 + BY24)@1	95.36%@8h	0.309	47.54	2.20	0.991

Table S4 Photodegradation efficiencies of **(MB+BY24+BR14)@1** towards RB21 after five photocatalytic cycles.

Cycle	1de (%)	2de (%)	3de (%)	4de (%)	5de (%)
RB21	96.07	93.63	89.99	87.2	81.03

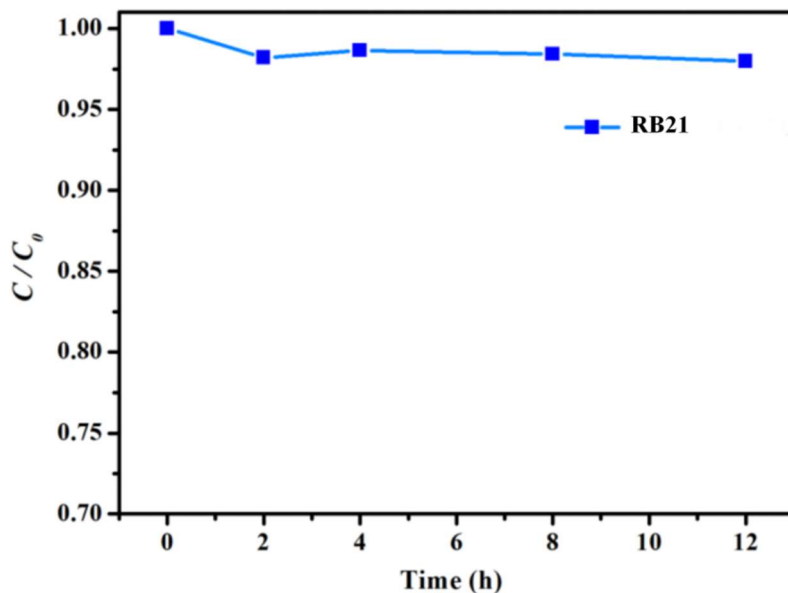


Fig. S12 The concentration variations of RB21 aqueous solution under visible-light in the absence of **1**.

Section S14 COD_{cr} determinations

Table S5 COD_{cr} values for the residual RB21 dye solutions after photocatalytic degradation.

Catalysts	COD _{cr} (mg L ⁻¹) Original	COD _{cr} (mg L ⁻¹) Residual	Efficiency (%) COD _{cr}	Efficiency (%) Degradation
RB21/1	805.50	165.13	79.50	73.13
MB@1	805.50	99.97	88.95	91.37
BR14@1	805.50	110.29	86.31	88.76
BY24 @1	805.50	480.62	40.33	40.99
(MB+BR14)@1	805.50	603.64	25.06	33.87
(MB+BY24)@1	805.50	70.94	91.19	93.10
(BR14+BY24)@1	805.50	101.61	87.39	89.98
(MB+BR14+BY24)@1	805.50	35.56	95.59	95.36

Section S15 References

1. R. Gangwar, S. Rasool and S. Mishra, *Biotechnol. Rep.*, 2016, **12**, 52–61.
2. M. C. Silva, A. D. Corrêa, M. T. S. P. Amorim, P. Parpot, J. A. Torres and P. M. B. Chagas, *J. Mol. Catal. B: Enzym.*, 2012, **77**, 9–14.
3. S. M. A. G. U. Souza, E. Forgiarini and A. A. U. Souza, *J. Hazard. Mater.*, 2007, **147**, 1073–1078.
4. T. Kenzom, P. Srivastava and S. Mishra, *Appl. Environ. Microbiol.*, 2014, **80**, 7484–7495.
5. I. Arslan and I. A. Balcioğlu, *Dyes Pigm.*, 1999, **43**, 95–108.
6. T. Marchis, P. Avetta, A. Bianco-Prevot, D. Fabbri, G. Viscardi and E. Laurenti, *J. Inorg. Biochem.*, 2011, **105**, 321–327.
7. A. Conneely, W.F. Smyth and G. McMullan, *FEMS Microbiol. Lett.*, 1999, **179**, 333–337.
8. R. D. Matthews, L. A. Bottomley and Spyros. G. Pavlostathis, *Desalination*, 2009, **248**, 816–825.
9. E. Haque, J. W. Jun and S. H. Jhung, *J. Hazard. Mater.*, 2011, **185**, 507–511.
10. W. Q. Kan, B. Liu, J. Yang., Y. Y. Liu and J. F. Ma, *Cryst. Growth Des.*, 2012, **12**, 2288–2298.
11. Q. Liu., H. J. Cong and H. X. Deng, *J. Am. Chem. Soc.*, 2016, **138**, 13822–13825.
12. H. Zhang, K Yu, J. H. Lv, L. H. Gong, C. M. Wang, C. X. Wang, D. Sun and B. B. Zhou, *Inorg. Chem.*, 2015, **54**, 6744–6757.